Title

Probing the correlation of neuronal loss, neurofibrillary tangles, and cell death markers across the Alzheimer's disease Braak stages: a quantitative study in humans

Authors

Theofilas, Panos
Ehrenberg, Alexander J
Nguy, Austin
et al.

Publication Date

2018

DOI

10.1016/j.neurobiolaging.2017.09.007

Peer reviewed

HHS Public Access

Author manuscript

Neurobiol Aging. Author manuscript; available in PMC 2019 January 01.

Published in final edited form as:

Neurobiol Aging. 2018 January ; 61: 1–12. doi:10.1016/j.neurobiolaging.2017.09.007.

Probing the correlation of neuronal loss, neurofibrillary tangles and cell death markers across the Alzheimer's disease's Braak stages: a quantitative study in humans

Panos Theofilas, PhD[1], **Alexander J. Ehrenberg**[1], **Austin Nguy**[1], **Julia M. Thackrey**[1], **Sara Dunlop, BS**[1], **Maria B. Mejia, BS**[1], **Ana T. Alho, PhD**[2,3], **Renata Elaine Paraizo Leite, PhD**[4], **Roberta Diehl Rodriguez, MD**[3], **Claudia K. Suemoto, MD, PhD**[4], **Camila F. Nascimento, PhD**[3], **Marcus Chin**[5], **Daniel Medina-Cleghorn, PhD**[5], **Ana Maria Cuervo, MD, PhD**[6], **Michelle Arkin, PhD**[5], **William W. Seeley, MD, PhD**[1], **Bruce L. Miller, MD**[1], **Ricardo Nitrini, MD, PhD**[7], **Carlos Augusto Pasqualucci, MD, PhD**[3], **Wilson Jacob Filho, MD, PhD**[4], **Udo Rueb, MD, PhD**[8], **John Neuhaus, PhD**[9], **Helmut Heinsen, MD, PhD**[3,10], and **Lea T. Grinberg, MD, PhD**[1,3]

[1]Memory and Aging Center, Department of Neurology, University of California, San Francisco, San Francisco, CA, USA

[2]Hospital Albert Einstein, São Paulo, Brazil

[3]Department of Pathology, LIM-22, University of São Paulo Medical School, São Paulo, Brazil

[4]Division of Geriatrics, LIM-22, University of São Paulo Medical School, São Paulo, Brazil

[5]Department of Pharmaceutical Chemistry, University of California, San Francisco, San Francisco, CA, USA

[6]Depts. of Developmental and Molecular Biology, Anatomy and Medicine, Albert Einstein College of Medicine, Bronx, NY, USA

[7]Department of Neurology, University of São Paulo Medical School, São Paulo, Brazil

[8]Dr. Senckenbergisches Chronomedizinisches Institut, J. W. Goethe University Frankfurt am Main, Germany

[9]Department of Epidemiology & Biostatistics, University of California, San Francisco, San Francisco, CA, USA

[10]Department of Psychiatry, University of Wuerzburg, Wuerzburg, Germany

Abstract

Clarifying the mechanisms connecting NFT neurotoxicity to neuronal dysfunction in humans are likely to be pivotal for developing effective treatments for Alzheimer's disease. To model the

Corresponding author: Lea Tenenholz Grinberg, MD/PhD, Associate Professor in Residence, Memory and Aging Center, Department of Neurology, Sandler Neurosciences Center, Box 1207, 675 Nelson Rising Lane, Room 211B, San Francisco, CA 94158, Phone: 415-502-7174, Fax: 415-476-5573.

temporal progression of AD in humans, we used a collection of brains with controls and individuals from each Braak stage to quantitatively investigate the correlation between intraneuronal caspase activation or macroautophagy markers, NFT burden and neuronal loss, in the dorsal raphe and locus coeruleus, the earliest vulnerable areas to NFT accumulation. We fit linear regressions with each count as outcomes, with Braak score and age as the predictors. In progressive Braak stages, intraneuronal aCasp-6 positivity increases both alone and overlapping with neurofibrillary tangles (NFT). Likewise, the proportion of NFT bearing neurons showing autophagosomes increases. Overall, caspases may be involved in upstream cascades in AD, and are associated with higher NFTs. Macroautophagy changes correlate with increasing NFT burden from early AD stages.

Keywords

Alzheimer's disease; neurofibrillary tangles; caspases; autophagy; neuron counts; human brainstem

1. Introduction

Alzheimer's disease (AD) features positive (β-amyloid neuritic plaques and phosphorylated-tau neurofibrillary tangles - NFTs) and negative (neuronal and synaptic loss) lesions (Duyckaerts et al., 2009). Since the late 1980s, when virtually every autosomal dominant AD cases have been linked to mutations in genes involved with amyloid precursor protein (APP) processing, the conventional view on AD pathogenesis places β-amyloid deposition as a central etiological event driving a cascade of pathological events resulting in neuronal loss (Hardy, 2017). However, the massive failure of clinical trials focusing on modulating the amyloid cascade put in check the amyloid hypothesis (Korczyn, 2012, Ricciarelli and Fedele, 2017).

Although AD-related neuropathogenic mechanisms remain elusive, and disease-modifying treatments are still unavailable numerous independent studies demonstrated that neuronal and synaptic loss are the best predictors of cognitive decline, (Andrade-Moraes et al., 2013, Arendt, 2009, Coleman et al., 2004, DeKosky and Scheff, 1990, Giannakopoulos et al., 2009, Terry et al., 1991), therefore, interventions targeting pathways involved in AD-related neuronal loss are likely to be critical.

Interestingly, autopsy and molecular imaging studies failed to demonstrate a good correlation between distribution and burden of β-amyloid plaques and cognitive scores. On the other hand, the spread of NFTs through neuronal networks, best represented by Braak staging system (BB)(Braak and Braak, 1991), has a strong correlation to neuronal loss and cognitive decline (Giannakopoulos et al., 2009, Suemoto et al., 2017). The BB system that initially included cortical areas only (BB 1 to 6), and revisited in 2011 to include brainstem structures in which NFT formation precedes cortical NFTs (BB 0 a–c) (Braak et al., 2011, Grinberg et al., 2009), is the highly reproducible both in autopsy as in longitudinal tau PET imaging studies (Scholl et al., 2016), suggesting that NFT formation is involved in processes culminating in neuronal death (Gomez-Isla et al., 1997, Iqbal et al., 2009). Thus, clarifying

the mechanisms connecting NFT neurotoxicity to neuronal dysfunction is likely to be pivotal for developing effective treatments.

Among the cell death pathways linked to NFT formation, caspase (Casp)-dependent and autophagy pathways have been implicated in AD pathophysiology, (Cotman and Su, 1996, Cotman et al., 2005, de Calignon et al., 2010, Dickson, 2004, Guo et al., 2004, LeBlanc et al., 2014, Martinez-Vicente and Cuervo, 2007, Piras et al., 2016, Rohn and Head, 2008). In experimental models of AD, active caspases (aCasp), including active caspase-6 (aCasp-6), are the best inductors of neuronal cell death (Zhang et al., 2000) and are also linked to upstream events leading to the formation of NFTs and β-amyloid plaques (Albrecht et al., 2007, de Calignon et al., 2010, Hyman and Yuan, 2012, Murray and Renslo, 2013). Specifically, by truncating tau, active effector caspases can create cleaved-tau species that are prone to aggregation and toxicity (de Calignon et al., 2010, LeBlanc, 2005). In fact, higher levels of Casp cleaved tau in the cerebrospinal fluid correlates with AD severity (Ramcharitar et al., 2013). For a thorough review of caspases and their role in neurodegenerative diseases, please see Shalini et al. 2015 (Shalini et al., 2015), LeBlanc 2013 (LeBlanc, 2013) and Graham et al. 2011 (Graham et al., 2011). Autophagy, a highly regulated process responsible for the breakdown of misfolded or aggregated proteins in healthy cells, becomes dysfunctional in AD models and fails to degrade toxic abnormal tau species potentially contributing to neuronal death (Martinez-Vicente and Cuervo, 2007, Nixon et al., 2005, Nixon, 2013, Piras et al., 2016, Vilchez et al., 2014, Wong and Cuervo, 2010)

However, despite this large body of literature derived from experimental models, attempts to validate these findings in human tissue were mostly restricted to semi-quantitative or qualitative studies comparing controls versus severe AD, and little is known about the co-occurrence of markers of specific cell death pathways with NFTs or with neuronal loss or at which point of AD temporal progression such pathways are activated.

Hypothesizing that changes in caspase-dependent and autophagic pathways occur from early AD stages and correlated with increased tau burden along AD progression in humans, we conducting a study using double-stained immunofluorescence and quantitative methods to investigate how early in AD progression Casp-6 and autophagy are activated, and their relationship to NFT burden and neuronal loss along AD neuropathological progression. This study innovates by focusing on the dorsal raphe nucleus (DRN), a serotonin-producing nucleus in the midbrain, and locus coeruleus (LC), a noradrenergic nucleus located in the pons (Figure 1) show the earliest vulnerability to accumulate tau cytoskeletal pathology in AD, prior to any cortical areas (Ehrenberg et al., 2017, Grinberg et al., 2009, Grudzien et al., 2007, Stratmann et al., 2015, Theofilas et al., 2017, Tomlinson et al., 1981) and degenerate progressively with AD increasing severity, thus representing a crucial intervention target in early AD stages when the neurons are still viable. Moreover, by employing a unique postmortem brainstem collection comprising controls (BB 0), early (BB stages I–II), intermediate (BB III–IV) and advanced (BB V–VI) AD (Braak and Braak, 1991). By comparing controls and individuals at well-defined progressive AD stages, our study design minimizes the inherent cross-sectional and descriptive nature of postmortem human studies by modeling the chain of events associated with AD progression that enables verifying the

translational relevance of results derived from experimental models, identification of relevant therapeutic targets and generation of testable hypothesis.

2. Materials and methods

2.1 Participants

The 24 cases included in this study (Table 1) were sourced from the Brain Bank of the Brazilian Brain Aging Study Group (BBBABSG) (Ferretti et al., 2010, Grinberg et al., 2007) and the Neurodegenerative Disease Brain Bank (NDBB) from the University of California, San Francisco (UCSF). All cases represented sporadic AD. The institutional review boards of both participating institutions approved this study. The BBBABSG is supplied by the São Paulo City Autopsy Service that performs approximately 13,000 autopsies per year. The selection criteria for this study included the absence of non-AD related neurodegenerative pathology or significant cerebrovascular lesions and availability of an intact brainstem. Subjects were excluded if they had a history of seizures, other neurological diseases, a primary Axis 1 psychiatric diagnosis (major mood disorders, psychotic disorders, and dissociative disorders), or gross non-degenerative structural pathology. For all cases, the neuropathological assessment was based on analysis of dementia-related structures, chosen according to the internationally accepted neuropathological guidelines, embedded in paraffin wax, cut into 8-micron thick sections, and stained with hematoxylin and eosin (H&E) and immunohistochemistry. BBBABSG (Grinberg et al., 2007) and NDBB neuropathological protocols are similar. AD pathology was staged according to the new NIA-AA guidelines (Montine et al., 2012). Cases were categorized according to the BB staging system for NFT changes (Braak and Braak, 1991). Subjects were considered to be BB stage 0 or free of cortical NFTs when at least four sections across the transentorhinal cortex were negative for phospho-tau immunostaining (phospho-tau antibody CP-13, 1:500, gift of Peter Davies) (Grinberg et al., 2009). All selected cases have a postmortem interval of less than 20 hs (average: 13 h 30 min).

2.2 Tissue processing and staining

Tissue processing and staining protocols have been described previously (Theofilas et al., 2014). In summary, the brainstem was severed from the brain and cerebellum. The brainstem was then immersed in 10% buffered formalin and fixed for at least six months., followed by embedding in 8% celloidin for subsequent sectioning (Heinsen et al., 2000). Blocks were sectioned horizontally in serial sets, each one containing one 300-μm thick and five 60-μm thick sections (Theofilas et al., 2014). The markers of interest were estimated in 60-μm thick sections, at equidistant intervals of 1200 μm, covering the whole region of interest (ROI) (an average of six sections per ROI). For cytoarchitectonic visualization of the LC and DRN neurons and for tracing the nuclei borders, all thick odd-numbered sections covering the entire ROI were gallocyanin (Nissl) stained (Sigma-Aldrich).

Sections were autoclaved in citrate buffer retrieval solution for 5 min at 121 °C, followed by 30 min incubation with 0.1% Sudan Black B (Sigma-Aldrich) for blocking autofluorescence and 30 min incubation in protein blocking solution with 5% milk in phosphate-buffered saline with 0.05% Tween 20 (PBS-T) at room temperature (RT). The antibody CP-13 (tau

serine 202) was used to detect NFTs in combination with two surrogate markers of pathways involved in neuronal death: active caspase-6, and the microtubule-associated protein, 1A/1B-light chain-3, (LC3)-positive (+) puncta. LC3, a mammalian homolog of yeast Atg8; was used as an autophagosome and macroautophagy marker (Kadowaki and Karim, 2009, Rosenfeldt et al., 2012). Lack of an antibody against aCasp-6 for immunohistochemical assays in human brain tissue led us to select a polyclonal antibody (Table 2). Information and experiments conducted to assure the specificity of the antibodies of choice are provided as Supplementary Material, including Figure S2.

Double immunofluorescence (CP-13/LC3 or CP-13/aCasp-6 - Table 2) was performed overnight at 4 °C in PBS, followed by incubation with immunofluorescence anti-rabbit secondary antibodies conjugated to Alexa Fluor 488 and anti-mouse secondary antibodies conjugated to Alexa Fluor 546 for 1h at RT (1:200 in PBS-T; A-11008 and A-11003 respectively, both by Invitrogen, CA). Neuronal cell bodies were labeled with (4′,6-Diamidino-2-Phenylindole, Dihydrochloride) DAPI contained in the mounting medium (Vector Labs). Negative control staining was performed by substituting each primary antibody for PBS-T. A positive control section was included in each batch. For checking the staining quality and the characteristics of the marker in the tissue, the sections were photographed with a Nikon Ti-E Microscope/Yokagawa CSU22 spinning disk confocal, using Plan Apo 40x/0.95 Corr and VC 60x/1.4 Oil objectives, and images were processed using Micro-Manager software 1.4 (Edelstein et al., 2014). For subsequent quantitative analyses, the sections were photographed with a Nikon 6D high-throughput widefield epifluorescence microscope (Nikon, Tokyo, Japan). Each ROI was imaged at 10x magnification (Plan Apo 10x/0.45, Nikon, Japan), and each image set covering the ROIs were merged into a single composite using NIS-Elements 4.30 (Nikon, Japan).

2.3 Quantitative analyses of the markers of interest

In each composite image, ROI boundaries were traced using cytoarchitectonic parameters based on Olszewski and Baxter (Olszewski and Baxter, 1982). Brainstem sections containing the DRN were collected from the level of the caudal border of the inferior colliculus, through the caudal pole of the oculomotor complex (III), a distance of about 6 mm. On cross-section, the rostral DRN borders encompass a fountain-shaped cell group composed of a medially situated central portion and two lateral wings. We traced the central portion between the medial longitudinal fasciculus (MLF) of each side and its dorsal extend to the base of the cerebral aqueduct. We traced the lateral wings dorsally to the MLF and the trochlear nuclei.

Brainstem sections containing the LC were collected caudally from the level of the dorsal oral pole of the motor trigeminal nucleus to the level of the caudal border of the inferior colliculus, a distance of approximately 12 mm. We traced the LC borders dorsomedially to the central gray matter, dorsolaterally to the mesencephalic trigeminal nucleus, ventrally and ventromedially to the nucleus reticularis pontis oralis. Although the ROI borders were distinguishable in the IF image compositions, we confirmed the tracers in each adjacent gallocyanin-stained thick section. Adobe Photoshop CS6 built-in counting tool (Adobe, CA) was used for manual cell counting. Neurons were classified by type and presence of

phospho-tau inclusions (Table 3). Photoshop's built-in counting tool tracked the number of markers per group. Counting was conducted on merged images and confirmed on single channel images, for precision. For each marker, final numbers were calculated as an average of all the sections covering each ROI (DRN and the unilateral LC).

2.4 Statistical Analyses

We assessed the association of BB stage and cell counts by generating plots and fitting a linear regression model for each estimation. The dependent variables for the models were the total estimated neuronal population for a certain marker or combination of markers (NFT + only, aCasp-6 or LC3 + only, and both NFT/aCasp-6 or LC3 positive) and the proportion of neurons positive for each of these markers or combination of markers (total number of positive neurons divided by total estimated neuronal numbers), for the DRN and LC with BB stage and age as the predictors. The estimated regression coefficients from these models measured the age-adjusted difference in the proportion of cells positive between individuals who differ by one BB stage. We fit the linear regression models and produced the plots using routines in the Stata software package (Stata Statistical Software v14, StataCorp, TX) and R (R Development Core Team; www.r-project.org). Results from the statistical analyses are summarized in Supplementary Table S1.

3. Results

Table 1 depicts demographics and neuropathological data of all 24 cases (54% females; mean age at death: 65.6 ± 12.2 years, range 44 to 88 years old).

3.1 Experiments on caspase and NFT: The LC and DRN show a higher number of neurons positive for active Caspase-6 positivity for each increment of the Braak and Braak (BB) stage

Neuronal counts were based on each of the four experimental groups (Table 3 – upper row) in the DRN and the LC of subjects at progressive stages of the AD pathological spectrum.

We identified few aCasp-6 + only neurons (experimental group 1) in controls (BB stage 0). Their numbers increased significantly with BB stage increment in the DRN (β=4.747; p=0.001; 95% CI [2.146, 7.349]; Figure 2A) and the LC (β=0.664; p<0.001; 95% CI [0.316, 1.012]; Figure 3A). The association between aCasp-6 + only neurons and AD severity remained significant after adjusting for age in DRN (β= 6.913; p<0.001; 95% CI [3.846, 9.979]) and LC (β= 0.693; p=0.005; 95% CI of [0.233, 1.153]). Neurons positive for both NFTs and aCasp-6 (experimental group 3) were also detected in cases at BB stage 0 and their numbers significantly increased with BB stage increment in the DRN (unadjusted: (β= 2.096; p<0.001; 95% CI [1.026, 3.166]); adjusted: (β= 2.874; p<0.001; 95% CI [1.575, 4.174]; Figure 2C) and the LC (unadjusted: β=0.316; p=0.01; 95% CI [0.082, 0.550]; Figure 3C). The correlation loss significance after adjusting for age in the LC (β=0.254; p=0.099; 95% CI [−0.053, 0.560]).

Because AD progression is associated with neuronal loss, comparing the average total numbers of neurons in each Braak stage may be misleading. Therefore, we analyzed the proportion of neurons bearing tau inclusions, aCasp-6, or both in each Braak stage (number

of neurons in a given group divided by the sum of neurons; Table S1). Once again, we detected a significant increase on the proportion of aCasp-6 + only neurons per BB stage increment in the DRN (β=2.387; p=0.007; 95% CI [0.723, 4.050]; Figure 2D (squares) and the LC (β=1.883; p<0.001; 95% CI [1.292, 2.473]; Figure 3D (squares). The association remained strong after adjusting for age (DRN: β=4.027; p<0.001; 95% CI [2.171, 5.883], and LC: β=2.395; p<0.001; 95% CI [1.707, 3.084]). The proportion of neurons positive for both NFTs and aCasp-6 significantly increased with AD severity in the DRN (unadjusted: β=1.04; p=0.004; 95% CI [0.366, 1.713]; adjusted: β=1.698; p<0.001; 95% CI [0.944, 2.452]; Figure 2D (triangles) and the LC (unadjusted: β=0.844; p<0.001; 95% CI [0.472, 1.217]; adjusted: β=0.984; p<0.001; 95% CI [0.501, 1.467]; Figure 3D (triangles). In summary, we observed increased absolute and relative burden of aCasp-6 + only, NFT + only, and neurons positive for both markers along AD progression.

3.2 Experiments on macroautophagy and NFTs: Co-localization of LC3 and NFT in the LC and DRN increases with BB stage

Following the same quantitative approach described above, we estimated the neuronal population and the proportion of neurons bearing the markers of interest in each Braak stage group Table 3 – bottom row). We detected a significant negative correlation between the number of neurons with LC3 + only (group 1) and increased BB stage in the DRN (β= −12.57; p=0.005; 95% CI [−20.86, −4.29] and LC (β=−6.01; p<0.001; 95% CI [−8.83, −3.19]) (Figures 4A and 5A, respectively). After adjusting for age, the association remained significant in the DRN (β=−11.72; p=0.0369; 95% CI [−22.66, −0.78] and the LC (β= −6.356; p=0.002; 95% CI [−10.07, −2.64]. As opposed to LC3 + only neurons, the number of neurons positive for both LC3 puncta and NFT (group 3) were positively correlated to AD severity in the DRN (β=1.51; p=0.004; 95% CI [0.528, 2.493]), and the LC (β=0.38; p=0.016; 95% CI [0.076, 0.684]) (Figures 4C and 5C, respectively). After adjusting for age, the association remained significant in the DRN (β=2; p=0.003; 95% CI [0.75, 3.25] but lost significance in the LC (β=0.394; p=0.054; 95% CI [−0.008, 0.795]. When examining the proportion of neurons containing both LC3 puncta and NFT over the total number of neurons, we observed a significant positive correlation with AD severity in the DRN (unadjusted: β=1.084; p=0.002; 95% CI 0.43, 1.74]; adjusted: β=1.69; p<0.001; 95% CI [0.94, 2.44]; Figure 4D (square), and the LC (unadjusted: β=1.09; p=0.003; 95% CI [0.4, 1.78]; adjusted: β=1.61; p<0.001; 95% CI [0.78, 2.44]; Figure 5D (square).

On the other hand, we did not observe any significant correlations with respect to the proportion of LC3+ only neurons in the DRN (unadjusted: β=−3.16; p=0.058; 95% CI [−6.44, 0.12], adjusted for age: β=−2.27; p=0.284; 95% CI [−6.56, 2.02]; Figure 4D (triangle) or in the LC (unadjusted: β=−2.26; p=0.121; 95% CI [−5.17, 0.65], adjusted for age: β=−1.83; p=0.332; 95% CI [−5.67, 2.01]; Figure 5D (triangle).

4. Discussion

In this study, we used a collection of well-characterized postmortem brains from individuals with sporadic AD including control, early, intermediate, and advanced BB stages to analyze two protein markers related to neuronal death in AD: aCasp-6 (Figure 6) and the

macroautophagy marker LC3 (Figure 7). We examined whether and how early these markers were detectable in aminergic brainstem nuclei extremely vulnerable to AD, how their burden changed during disease progression, and to which degree they were expressed in NFT bearing neurons.

By investigating the full extent of DRN and LC from 24 subjects free from non-AD-related pathology, we demonstrate that: (1) elderly controls (BB 0) showed intra-neuronal Casp-6 activity in the DRN and LC in a small percentage of neurons. The number of aCasp-6 bearing neurons progressively increased both in absolute and relative terms during AD neuropathological progression (Figures 2 and 3); (2) the same pattern of neurons bearing both aCasp-6 and NFTs, although in the LC, only the relative numbers increased (Figure 3D); (3) Control individuals (BB 0) showed high absolute numbers of neurons bearing LC3 puncta only in the DRN and LC; (4) Neurons bearing LC3 puncta decreased in number during AD progression, whereas the number of NFT + only neurons increased. (5) The absolute and relative numbers of neurons positive for NFT and LC3 increased (Figures 4 and 5). In the DRN and LC, the relative numbers of LC3 + only neurons did not change during the disease progression (Figures 4 and 5).

aCasp-6 is traditionally classified as an apoptotic effector (D'Amelio et al., 2012, Graham et al., 2011, Julien et al., 2016, Rohn and Head, 2008) that induces a successive disassembly of cells by targeting critical cellular proteins including structural and DNA repair proteins, functions that confirm its role as an independent executioner of apoptosis (Ruchaud et al., 2002, Slee et al., 2001). For example, aCasp-6 ablated neurons were protected against excitotoxic insults, trophic factor withdrawal, and axonal degeneration (Uribe et al., 2012). Additionally, aCasp-6 is integral in non-apoptotic related cascades, including axonal pruning during development (Simon et al., 2012), and axonal degeneration in pathological conditions (Akpan et al., 2011). aCasp6 activity may contribute to cell loss mechanisms in AD but its activation could be reversible, thus its exact role remains unclear (Graham et al., 2011).

Several studies support aCasp-6 as a pro-apoptotic mediator of cell death in AD (Wang et al., 2015). Klaiman et al. (2008) demonstrated in primary human neuronal protein extracts that aCasp-6 cleaves important cytoskeletal-associated proteins including α-tubulin, which is also found to be cleaved by aCasp-6 in neurons from AD brains (Albrecht et al., 2007, Guo et al., 2004, Klaiman et al., 2008). This suggests a role of aCasp-6 in the modulation of neuronal cytoskeleton network and function. Moreover, Albrecht et al. (2007) showed Casp–mediated tau cleavage in pre-tangles in the human hippocampus, while levels of Casp-cleaved tau and NFTs correlated inversely with global cognitive scores, suggesting that cascades involving Casp activation are highly relevant to AD pathogenesis (Albrecht et al., 2007). Also, in support of the hypothesis that Casp-6 activation precedes NFT formation, de Calignon et al. (2010) demonstrated that Casp-6 activation preceded NFT formation in a model of tauopathy (P301L tau transgenic Tg4510 mice) (de Calignon et al., 2010). On the other hand, Caps-6 activation does not necessarily result in apoptosis, suggesting that aCasp-6 may be involved in upstream events. For example, Klaiman et al. (2009) failed to observe mitochondrial dysfunction and neuronal death after Casp-6 overexpression in cultured cells despite the presence of high levels of Casp-6 activity (Klaiman et al., 2009). Furthermore, Zhang et al. (2000) demonstrated that microinjection of recombinant aCasp-6

in the cytosol of human primary neurons failed to induce rapid cell death (Zhang et al., 2000). These neurons showed TUNEL-positivity only after a delay of 2–8 days. In one of the few studies in human brains, Guo et al. (2004) showed that neurons bearing aCasp-cleaved tau had normal nuclear morphology, in the absence of apoptosis or another type of cell death, despite a strong aCasp-6 presence primarily in NFT and neurites (Guo et al., 2004). Finally, the interplay of aCasp-6 and tau may go beyond AD. Guillozet-Bongaarts et. al detected aCasp-6-cleaved tau in Pick's bodies but not in tau astrocytic inclusions in progressive supranuclear palsy and corticobasal degeneration (Guillozet-Bongaarts et al., 2007).

Here we tested if Casp-6 activation (Figure 6) occurs upstream rather than being an end-stage event that may lead to apoptotic cell death in humans with AD. Should aCasp-6 be only involved in end-stage apoptosis, we would expect aCasp-6 and TUNEL positivity in the LC and DRN only in brains from mid-disease stages (BB stage ≥ III), when the neuronal loss is prominent (Ehrenberg et al., 2017, Theofilas et al., 2017). However, our study identified aCasp-6 positivity as an early event in AD, in neurons with and without NFTs and only partially overlapping with TUNEL staining (Figure S1). The increase of aCasp-6 positivity was rather linear, following a gradual higher burden of NFT lesions across the BB stages, but only with moderate overlapping with NFTs. This finding suggests that aCasp-6 could operate upstream with a broader role in neurodegeneration, rather than being a direct inducer of apoptosis in NFT + neurons. The cross-sectional nature of this study precludes investigating whether NFT + only neurons represent cells with concomitant Casp activation. The presence of aCasp-6 only neurons is intriguing, and the lack of NFT could be related to specific neuronal vulnerability, including differential expression of the presence of the co-chaperone C-terminus of the Hsc70-interacting protein (CHIP). CHIP is critical for degrading Casp-cleaved tau (Dolan and Johnson, 2010) and contributes to the regulation of Casp activity (Saidi et al., 2015). In CHIP knockout mice, Casp-cleaved tau levels are increased (Dickey et al., 2006). Also, pseudo-phosphorylation of tau Serine 422 inhibits tau truncation mediated by caspases *in vitro* (Guillozet-Bongaarts et al., 2006). Further studies exploring the relationship between Casp-6 activation, neuronal survival in neurons with or without CHIP and overlapping tau species phosphorylated at serine 422 along the AD progression may shed light on this question.

The autophagy-lysosome pathway is one of two major systems responsible for degrading the cellular material and misfolded proteins, the other being the ubiquitin-proteasome system (Choi et al., 2013, Goldberg, 2003). During macroautophagy, the major lysosomal degrading pathway, cytoplasmic cargo is sequestered within autophagosomes, identified by the well-established membrane marker LC3 that regulates the autophagosome formation and remains linked to the mature autophagosome membrane (Klionsky et al., 2008). The significance of macroautophagy in clearance of phospho-tau is supported by observations in transgenic models. Inactivation of autophagy-related protein (Atg) gene *Atg7* in adult Atg7 conditional knockout mouse brains increased pathological accumulation of phospho-tau protein, suggesting a role of macroautophagy in reducing phospho-tau accumulation in affected neurons (Inoue et al., 2012). Inhibition of macroautophagy via cathepsin-mediated proteolysis within autolysosomes in primary cortical neurons from rat brains led to a marked accumulation of autophagosomes containing cathepsin D and incomplete degraded LC3.

This phenotype was also observed in neurons with AD pathology, suggesting that autophagy deficiency and accumulation of autophagosomes/LC3 containing partially digested autophagic substrates in the AD most likely arises from impaired clearance of autophagosomes in AD and other tauopathies (Boland et al., 2008, Choi et al., 2013, Lee et al., 2010, Piras et al., 2016, Wolfe et al., 2013). Defective clearance of processed tau by the autophagy-lysosome system mediates tau aggregation and AD-like pathology in animal models of AD (Hara et al., 2006, Komatsu et al., 2006, Pickford et al., 2008). Moreover, pharmacological induction of autophagy in tauopathy mouse models promoted tau clearance and was associated with reduced LC3 positivity, tau hyperphosphorylation, and improved neuronal survival (Ozcelik et al., 2013, Schaeffer et al., 2012).

Using immunostaining in human postmortem brains from patients with primary tauopathies and familiar AD, Piras et al. (2016) detected increased levels of LC3-positive puncta and autophagic vesicle accumulation in the frontal cortex, suggesting a defect in the autophagosome pathway that could underline pathological tau accumulation (Piras et al., 2016). In line with these findings, electron microscopy studies on neocortical biopsies from AD brains detected autophagy induction and accumulation of autophagosomes containing undigested autophagic substrates, possibly due to defective autophagosomal maturation in AD neurons resulting in failure of protein clearance {{; 88 Nixon 2005}}. Taken together, these observations provide evidence that macroautophagy is extensively involved in the AD pathogenesis, and is closely related to autophagosome upregulation (LC3 puncta) as a possible compensatory mechanism to increase autophagy in the affected neurons.

Here, we investigated the presence of active macroautophagy using LC3 immunoreactivity in the form of cytoplasmic puncta as a surrogate marker (Figure 7). We observed that following BB stage progression, the presence of LC3 in NFT negative neurons decreased significantly, whereas a higher proportion of NFT + neurons showed LC3 positive puncta. Although our study was not meant to test if LC3 positive puncta were functional or not, our findings revealed a general failure of macroautophagy along BB stage progression, possibly linked to NFT accumulation. For example, accumulation of cytoplasmic phospho-tau could be related to impaired tau degradation by the autophagosome system as found in studies where the accumulation of autophagic vesicles overlapped with defective lysosomal clearance in AD and other tauopathies.

Further studies in human brains investigating the co-occurrence of autophagy markers, Casp-related tau cleavage, and abnormal tau immunostaining *in situ*, are crucial for determining whether these cascades act in the same neurons or represent parallel mechanisms that may lead to neuronal death in AD. Although multiplex immunostaining is limited by methodological hurdles such as species compatibility, promising new technologies, including improved primary conjugated antibodies and platforms replacing fluorophores by other detection methods (Angelo et al., 2014) will likely enable this line of studies.

This study has several strengths including: (1) a high-quality collection of well-characterized human brain samples enriched with individuals in the early stages of AD, that allows the study of BB stage progression in humans; (2) investigation of brainstem nuclei extremely

vulnerable to AD, across all Braak stages; (3) use of double-stained immunofluorescence to investigate the co-expression of the markers of interest and NFTs; and (4) use of quantitative methods for estimating the markers of interest providing less bias than traditional schemes limited to one brain section. On the other hand, this study comes with intrinsic limitations: (1) the BB staging system is a neuropathological marker of non-random spread of neurofibrillary tangles through brain networks. Although the BB staging system is deemed representative of AD progression based on numerous studies reproducing the findings, strong correlation with cognitive outcomes, and recent in vivo PET tau imaging studies supporting the postmortem findings (Scholl et al., 2016), it is important to note that the BB staging system is based on a cross-sectional study design, and it is rather a categorical than a continuous scale, (2) postmortem tissue studies have an inherent cross-sectional nature and are not suitable for mechanistic analysis of downstream markers that could further clarify involvement and interplay of the cell death pathways in inducing AD pathogenesis. For example, we can only postulate the long-term effects of aCasp-6 and LC3 activity in the same individuals as AD progresses. Nevertheless, the current step-wise approach is more informative than comparing controls and severe AD stages. (3) Relatively small sample size. Obtaining well-characterized postmortem human brain tissue is challenging, especially from controls and early-stage cases. Despite its relatively small size, our cohort is unique regarding the availability of the cases mentioned above and the entire ROIs for quantitative analyses. (4) Finally, despite our best efforts to include cases with minimum PMI, we cannot exclude the possibility that hypoxia-induced changes could influence cell death marker activity in our samples.

5. Conclusion

This study pioneers in showing progressive changes in aCasp-6 and macroautophagy positivity during the BB stage progression in humans, and their co-occurrence with NFT burden. We observed significant changes in aCasp-6 and LC3 markers positivity from early BB stages (BB I) despite the fact that neuronal loss is only evident in BB III (Ehrenberg et al., 2017, Theofilas et al., 2017), suggesting that tau-mediated- neuronal loss in humans with AD is multifactorial and characterised by an extensive gap between the activation of these pathways and neuronal loss. Due to the progressive nature of AD, interventions modulating caspase-activation and/or autophagy up-regulation may ameliorate tau burden and neuronal death in AD.

Supplementary Material

Refer to Web version on PubMed Central for supplementary material.

Acknowledgments

We thank the patients and their families for their invaluable contribution to brain aging neurodegenerative disease research, and the staff of the Sao Paulo Autopsy Service and BBBABSG for technical support. We thank Anita Spanova and Cristina Armas for their histological assistance and Daniel Medina-Cleghorn for assistance with cell cultures. This study was supported by the National Institutes of Health R01AG040311, P50AG023501, P01AG019724, K24AG053435, Alzheimer's Association (AARG-16-441514), the John Douglas French Alzheimer Foundation, UCSF - CTSI-Pilot Awards program, LIM-22/Faculdade de Medicina da Universidade de Sao Paulo, and Hospital Israelita Albert Einstein, Sao Paulo.

Abbreviations

aCasp	active caspases
AD	Alzheimer's disease
BB	Braak and Braak stage
BBBABSG	Brain Bank of the Brazilian Brain Aging Study Group
Casp	caspases
DRN	dorsal raphe nucleus
LC	locus coeruleus
LC3	microtubule-associated protein, 1A/1B-light chain-3
NDBB	Neurodegenerative Disease Brain Bank
NFT	neurofibrillary tangle
ROI	region of interest

References

Akpan N, Serrano-Saiz E, Zacharia BE, Otten ML, Ducruet AF, Snipas SJ, Liu W, Velloza J, Cohen G, Sosunov SA, Frey WH 2nd, Salvesen GS, Connolly ES Jr, Troy CM. Intranasal delivery of caspase-9 inhibitor reduces caspase-6-dependent axon/neuron loss and improves neurological function after stroke. J Neurosci. 2011; 31:8894–8904. [PubMed: 21677173]

Albrecht S, Bourdeau M, Bennett D, Mufson EJ, Bhattacharjee M, LeBlanc AC. Activation of caspase-6 in aging and mild cognitive impairment. Am J Pathol. 2007; 170:1200–1209. [PubMed: 17392160]

Andrade-Moraes CH, Oliveira-Pinto AV, Castro-Fonseca E, da Silva CG, Guimaraes DM, Szczupak D, Parente-Bruno DR, Carvalho LR, Polichiso L, Gomes BV, Oliveira LM, Rodriguez RD, Leite RE, Ferretti-Rebustini RE, Jacob-Filho W, Pasqualucci CA, Grinberg LT, Lent R. Cell number changes in Alzheimer's disease relate to dementia, not to plaques and tangles. Brain. 2013; 136:3738–3752. [PubMed: 24136825]

Angelo M, Bendall SC, Finck R, Hale MB, Hitzman C, Borowsky AD, Levenson RM, Lowe JB, Liu SD, Zhao S, Natkunam Y, Nolan GP. Multiplexed ion beam imaging of human breast tumors. Nat Med. 2014; 20:436–442. [PubMed: 24584119]

Arendt T. Synaptic degeneration in Alzheimer's disease. Acta Neuropathol. 2009; 118:167–179. [PubMed: 19390859]

Boland B, Kumar A, Lee S, Platt FM, Wegiel J, Yu WH, Nixon RA. Autophagy induction and autophagosome clearance in neurons: relationship to autophagic pathology in Alzheimer's disease. J Neurosci. 2008; 28:6926–6937. [PubMed: 18596167]

Braak H, Braak E. Neuropathological stageing of Alzheimer-related changes. Acta Neuropathol. 1991; 82:239–259. [PubMed: 1759558]

Braak H, Thal DR, Ghebremedhin E, Del Tredici K. Stages of the pathologic process in Alzheimer disease: age categories from 1 to 100 years. J Neuropathol Exp Neurol. 2011; 70:960–969. [PubMed: 22002422]

Choi AM, Ryter SW, Levine B. Autophagy in human health and disease. N Engl J Med. 2013; 368:1845–1846.

Coleman P, Federoff H, Kurlan R. A focus on the synapse for neuroprotection in Alzheimer disease and other dementias. Neurology. 2004; 63:1155–1162. [PubMed: 15477531]

Cotman CW, Poon WW, Rissman RA, Blurton-Jones M. The role of caspase cleavage of tau in Alzheimer disease neuropathology. J Neuropathol Exp Neurol. 2005; 64:104–112. [PubMed: 15751224]

Cotman CW, Su JH. Mechanisms of neuronal death in Alzheimer's disease. Brain Pathol. 1996; 6:493–506. [PubMed: 8944319]

D'Amelio M, Sheng M, Cecconi F. Caspase-3 in the central nervous system: beyond apoptosis. Trends Neurosci. 2012; 35:700–709. [PubMed: 22796265]

de Calignon A, Fox LM, Pitstick R, Carlson GA, Bacskai BJ, Spires-Jones TL, Hyman BT. Caspase activation precedes and leads to tangles. Nature. 2010; 464:1201–1204. [PubMed: 20357768]

DeKosky ST, Scheff SW. Synapse loss in frontal cortex biopsies in Alzheimer's disease: correlation with cognitive severity. Ann Neurol. 1990; 27:457–464. [PubMed: 2360787]

Dickey CA, Yue M, Lin WL, Dickson DW, Dunmore JH, Lee WC, Zehr C, West G, Cao S, Clark AM, Caldwell GA, Caldwell KA, Eckman C, Patterson C, Hutton M, Petrucelli L. Deletion of the ubiquitin ligase CHIP leads to the accumulation, but not the aggregation, of both endogenous phospho- and caspase-3-cleaved tau species. J Neurosci. 2006; 26:6985–6996. [PubMed: 16807328]

Dickson DW. Apoptotic mechanisms in Alzheimer neurofibrillary degeneration: cause or effect? J Clin Invest. 2004; 114:23–27. [PubMed: 15232608]

Dolan PJ, Johnson GV. A caspase cleaved form of tau is preferentially degraded through the autophagy pathway. J Biol Chem. 2010; 285:21978–21987. [PubMed: 20466727]

Duyckaerts C, Delatour B, Potier MC. Classification and basic pathology of Alzheimer disease. Acta Neuropathol. 2009; 118:5–36. [PubMed: 19381658]

Edelstein AD, Tsuchida MA, Amodaj N, Pinkard H, Vale RD, Stuurman N. Advanced methods of microscope control using muManager software. J Biol Methods. 2014; 1:e10. [PubMed: 25606571]

Ehrenberg AJ, Nguy AK, Theofilas P, Dunlop S, Suemoto CK, Alho AT, Leite RP, Diehl Rodriguez R, Mejia MB, Rub U, Farfel JM, de Lucena Ferretti-Rebustini RE, Nascimento CF, Nitrini R, Pasquallucci CA, Jacob-Filho W, Miller B, Seeley WW, Heinsen H, Grinberg LT. Quantifying the accretion of hyperphosphorylated tau in the locus coeruleus and dorsal raphe nucleus: the pathological building blocks of early Alzheimer's Disease. Neuropathol Appl Neurobiol. 2017

Ferretti RE, Damin AE, Brucki SMD, Morillo LS, Perroco TR, Campora F, et al. Post-Mortem diagnosis of dementia by informant interview. 2010; 4:138–144.

Giannakopoulos P, Kovari E, Gold G, von Gunten A, Hof PR, Bouras C. Pathological substrates of cognitive decline in Alzheimer's disease. Front Neurol Neurosci. 2009; 24:20–29. [PubMed: 19182459]

Goldberg AL. Protein degradation and protection against misfolded or damaged proteins. 2003; 426:899.

Gomez-Isla T, Hollister R, West H, Mui S, Growdon JH, Petersen RC, Parisi JE, Hyman BT. Neuronal loss correlates with but exceeds neurofibrillary tangles in Alzheimer's disease. Ann Neurol. 1997; 41:17–24. [PubMed: 9005861]

Graham RK, Ehrnhoefer DE, Hayden MR. Caspase-6 and neurodegeneration. Trends Neurosci. 2011; 34:646–656. [PubMed: 22018804]

Grinberg LT, Ferretti RE, Farfel JM, Leite R, Pasqualucci CA, Rosemberg S, Nitrini R, Saldiva PH, Filho WJ. Brazilian Aging Brain Study Group. Brain bank of the Brazilian aging brain study group - a milestone reached and more than 1,600 collected brains. Cell Tissue Bank. 2007; 8:151–162. [PubMed: 17075689]

Grinberg LT, Rub U, Ferretti RE, Nitrini R, Farfel JM, Polichiso L, Gierga K, Jacob-Filho W, Heinsen H. Brazilian Brain Bank Study Group. The dorsal raphe nucleus shows phospho-tau neurofibrillary changes before the transentorhinal region in Alzheimer's disease. A precocious onset? Neuropathol Appl Neurobiol. 2009; 35:406–416. [PubMed: 19508444]

Grudzien A, Shaw P, Weintraub S, Bigio E, Mash DC, Mesulam MM. Locus coeruleus neurofibrillary degeneration in aging, mild cognitive impairment and early Alzheimer's disease. Neurobiol Aging. 2007; 28:327–335. [PubMed: 16574280]

Guillozet-Bongaarts AL, Cahill ME, Cryns VL, Reynolds MR, Berry RW, Binder LI. Pseudophosphorylation of tau at serine 422 inhibits caspase cleavage: in vitro evidence and implications for tangle formation in vivo. J Neurochem. 2006; 97:1005–1014. [PubMed: 16606369]

Guillozet-Bongaarts AL, Glajch KE, Libson EG, Cahill ME, Bigio E, Berry RW, Binder LI. Phosphorylation and cleavage of tau in non-AD tauopathies. Acta Neuropathol. 2007; 113:513–520. [PubMed: 17357802]

Guo H, Albrecht S, Bourdeau M, Petzke T, Bergeron C, LeBlanc AC. Active caspase-6 and caspase-6-cleaved tau in neuropil threads, neuritic plaques, and neurofibrillary tangles of Alzheimer's disease. Am J Pathol. 2004; 165:523–531. [PubMed: 15277226]

Hara T, Nakamura K, Matsui M, Yamamoto A, Nakahara Y, Suzuki-Migishima R, Yokoyama M, Mishima K, Saito I, Okano H, Mizushima N. Suppression of basal autophagy in neural cells causes neurodegenerative disease in mice. Nature. 2006; 441:885–889. [PubMed: 16625204]

Hardy J. The discovery of Alzheimer-causing mutations in the APP gene and the formulation of the "amyloid cascade hypothesis". FEBS J. 2017; 284:1040–1044. [PubMed: 28054745]

Heinsen H, Arzberger T, Schmitz C. Celloidin mounting (embedding without infiltration) - a new, simple and reliable method for producing serial sections of high thickness through complete human brains and its application to stereological and immunohistochemical investigations. J Chem Neuroanat. 2000; 20:49–59. [PubMed: 11074343]

Hyman BT, Yuan J. Apoptotic and non-apoptotic roles of caspases in neuronal physiology and pathophysiology. Nat Rev Neurosci. 2012; 13:395–406. [PubMed: 22595785]

Inoue K, Rispoli J, Kaphzan H, Klann E, Chen EI, Kim J, Komatsu M, Abeliovich A. Macroautophagy deficiency mediates age-dependent neurodegeneration through a phospho-tau pathway. Mol Neurodegener. 2012; 7:48-1326-7-48. [PubMed: 22998728]

Iqbal K, Liu F, Gong CX, del Alonso AC, Grundke-Iqbal I. Mechanisms of tau-induced neurodegeneration. Acta Neuropathol. 2009; 118:53–69. [PubMed: 19184068]

Julien O, Zhuang M, Wiita AP, O'Donoghue AJ, Knudsen GM, Craik CS, Wells JA. Quantitative MS-based enzymology of caspases reveals distinct protein substrate specificities, hierarchies, and cellular roles. Proc Natl Acad Sci USA. 2016

Kadowaki M, Karim MR. Cytosolic LC3 ratio as a quantitative index of macroautophagy. Methods Enzymol. 2009; 452:199–213. [PubMed: 19200884]

Klaiman G, Champagne N, LeBlanc AC. Self-activation of Caspase-6 in vitro and in vivo: Caspase-6 activation does not induce cell death in HEK293T cells. Biochim Biophys Acta. 2009; 1793:592–601. [PubMed: 19133298]

Klaiman G, Petzke TL, Hammond J, Leblanc AC. Targets of caspase-6 activity in human neurons and Alzheimer disease. Mol Cell Proteomics. 2008; 7:1541–1555. [PubMed: 18487604]

Klionsky DJ, Abeliovich H, Agostinis P, Agrawal DK, Aliev G, Askew DS, Baba M, Baehrecke EH, Bahr BA, Ballabio A, Bamber BA, Bassham DC, Bergamini E, Bi X, Biard-Piechaczyk M, Blum JS, Bredesen DE, Brodsky JL, Brumell JH, Brunk UT, Bursch W, Camougrand N, Cebollero E, Cecconi F, Chen Y, Chin LS, Choi A, Chu CT, Chung J, Clarke PG, Clark RS, Clarke SG, Clave C, Cleveland JL, Codogno P, Colombo MI, Coto-Montes A, Cregg JM, Cuervo AM, Debnath J, Demarchi F, Dennis PB, Dennis PA, Deretic V, Devenish RJ, Di Sano F, Dice JF, Difiglia M, Dinesh-Kumar S, Distelhorst CW, Djavaheri-Mergny M, Dorsey FC, Droge W, Dron M, Dunn WA Jr, Duszenko M, Eissa NT, Elazar Z, Esclatine A, Eskelinen EL, Fesus L, Finley KD, Fuentes JM, Fueyo J, Fujisaki K, Galliot B, Gao FB, Gewirtz DA, Gibson SB, Gohla A, Goldberg AL, Gonzalez R, Gonzalez-Estevez C, Gorski S, Gottlieb RA, Haussinger D, He YW, Heidenreich K, Hill JA, Hoyer-Hansen M, Hu X, Huang WP, Iwasaki A, Jaattela M, Jackson WT, Jiang X, Jin S, Johansen T, Jung JU, Kadowaki M, Kang C, Kelekar A, Kessel DH, Kiel JA, Kim HP, Kimchi A, Kinsella TJ, Kiselyov K, Kitamoto K, Knecht E, Komatsu M, Kominami E, Kondo S, Kovacs AL, Kroemer G, Kuan CY, Kumar R, Kundu M, Landry J, Laporte M, Le W, Lei HY, Lenardo MJ, Levine B, Lieberman A, Lim KL, Lin FC, Liou W, Liu LF, Lopez-Berestein G, Lopez-Otin C, Lu B, Macleod KF, Malorni W, Martinet W, Matsuoka K, Mautner J, Meijer AJ, Melendez A, Michels P, Miotto G, Mistiaen WP, Mizushima N, Mograbi B, Monastyrska I, Moore MN, Moreira PI, Moriyasu Y, Motyl T, Munz C, Murphy LO, Naqvi NI, Neufeld TP, Nishino I, Nixon RA, Noda T, Nurnberg B, Ogawa M, Oleinick NL, Olsen LJ, Ozpolat B, Paglin S, Palmer GE, Papassideri I,

Parkes M, Perlmutter DH, Perry G, Piacentini M, Pinkas-Kramarski R, Prescott M, Proikas-Cezanne T, Raben N, Rami A, Reggiori F, Rohrer B, Rubinsztein DC, Ryan KM, Sadoshima J, Sakagami H, Sakai Y, Sandri M, Sasakawa C, Sass M, Schneider C, Seglen PO, Seleverstov O, Settleman J, Shacka JJ, Shapiro IM, Sibirny A, Silva-Zacarin EC, Simon HU, Simone C, Simonsen A, Smith MA, Spanel-Borowski K, Srinivas V, Steeves M, Stenmark H, Stromhaug PE, Subauste CS, Sugimoto S, Sulzer D, Suzuki T, Swanson MS, Tabas I, Takeshita F, Talbot NJ, Talloczy Z, Tanaka K, Tanaka K, Tanida I, Taylor GS, Taylor JP, Terman A, Tettamanti G, Thompson CB, Thumm M, Tolkovsky AM, Tooze SA, Truant R, Tumanovska LV, Uchiyama Y, Ueno T, Uzcategui NL, van der Klei I, Vaquero EC, Vellai T, Vogel MW, Wang HG, Webster P, Wiley JW, Xi Z, Xiao G, Yahalom J, Yang JM, Yap G, Yin XM, Yoshimori T, Yu L, Yue Z, Yuzaki M, Zabirnyk O, Zheng X, Zhu X, Deter RL. Guidelines for the use and interpretation of assays for monitoring autophagy in higher eukaryotes. Autophagy. 2008; 4:151–175. [PubMed: 18188003]

Komatsu M, Waguri S, Chiba T, Murata S, Iwata J, Tanida I, Ueno T, Koike M, Uchiyama Y, Kominami E, Tanaka K. Loss of autophagy in the central nervous system causes neurodegeneration in mice. Nature. 2006; 441:880–884. [PubMed: 16625205]

Korczyn AD. Why have we failed to cure Alzheimer's disease? J Alzheimers Dis. 2012; 29:275–282. [PubMed: 22258512]

LeBlanc AC. Caspase-6 as a novel early target in the treatment of Alzheimer's disease. Eur J Neurosci. 2013; 37:2005–2018. [PubMed: 23773070]

LeBlanc AC. The role of apoptotic pathways in Alzheimer's disease neurodegeneration and cell death. Curr Alzheimer Res. 2005; 2:389–402. [PubMed: 16248844]

LeBlanc AC, Ramcharitar J, Afonso V, Hamel E, Bennett DA, Pakavathkumar P, Albrecht S. Caspase-6 activity in the CA1 region of the hippocampus induces age-dependent memory impairment. Cell Death Differ. 2014; 21:696–706. [PubMed: 24413155]

Lee JH, Yu WH, Kumar A, Lee S, Mohan PS, Peterhoff CM, Wolfe DM, Martinez-Vicente M, Massey AC, Sovak G, Uchiyama Y, Westaway D, Cuervo AM, Nixon RA. Lysosomal proteolysis and autophagy require presenilin 1 and are disrupted by Alzheimer-related PS1 mutations. Cell. 2010; 141:1146–1158. [PubMed: 20541250]

Martinez-Vicente M, Cuervo AM. Autophagy and neurodegeneration: when the cleaning crew goes on strike. Lancet Neurol. 2007; 6:352–361. [PubMed: 17362839]

Montine TJ, Phelps CH, Beach TG, Bigio EH, Cairns NJ, Dickson DW, Duyckaerts C, Frosch MP, Masliah E, Mirra SS, Nelson PT, Schneider JA, Thal DR, Trojanowski JQ, Vinters HV, Hyman BT. National Institute on Aging Alzheimer's Association. National Institute on Aging-Alzheimer's Association guidelines for the neuropathologic assessment of Alzheimer's disease: a practical approach. Acta Neuropathol. 2012; 123:1–11. [PubMed: 22101365]

Murray J, Renslo AR. Modulating caspase activity: beyond the active site. Curr Opin Struct Biol. 2013; 23:812–819. [PubMed: 24215810]

Nixon RA. The role of autophagy in neurodegenerative disease. Nat Med. 2013; 19:983–997. [PubMed: 23921753]

Nixon RA, Wegiel J, Kumar A, Yu WH, Peterhoff C, Cataldo A, Cuervo AM. Extensive involvement of autophagy in Alzheimer disease: an immuno-electron microscopy study. J Neuropathol Exp Neurol. 2005; 64:113–122. [PubMed: 15751225]

Olszewski, J., Baxter, D. Cytoarchitecture of the human brain stem. 2. Karger; Basel; New York: 1982.

Ozcelik S, Fraser G, Castets P, Schaeffer V, Skachokova Z, Breu K, Clavaguera F, Sinnreich M, Kappos L, Goedert M, Tolnay M, Winkler DT. Rapamycin attenuates the progression of tau pathology in P301S tau transgenic mice. PLoS One. 2013; 8:e62459. [PubMed: 23667480]

Pickford F, Masliah E, Britschgi M, Lucin K, Narasimhan R, Jaeger PA, Small S, Spencer B, Rockenstein E, Levine B, Wyss-Coray T. The autophagy-related protein beclin 1 shows reduced expression in early Alzheimer disease and regulates amyloid beta accumulation in mice. J Clin Invest. 2008; 118:2190–2199. [PubMed: 18497889]

Piras A, Collin L, Gruninger F, Graff C, Ronnback A. Autophagic and lysosomal defects in human tauopathies: analysis of post-mortem brain from patients with familial Alzheimer disease, corticobasal degeneration and progressive supranuclear palsy. Acta Neuropathol Commun. 2016; 4:22-016-0292-9. [PubMed: 26936765]

Ramcharitar J, Albrecht S, Afonso VM, Kaushal V, Bennett DA, Leblanc AC. Cerebrospinal fluid tau cleaved by caspase-6 reflects brain levels and cognition in aging and Alzheimer disease. J Neuropathol Exp Neurol. 2013; 72:824–832. [PubMed: 23965742]

Ricciarelli R, Fedele E. The amyloid cascade hypothesis in Alzheimer's disease: it's time to change our mind. Curr Neuropharmacol. 2017

Rohn TT, Head E. Caspase activation in Alzheimer's disease: early to rise and late to bed. Rev Neurosci. 2008; 19:383–393. [PubMed: 19317178]

Rosenfeldt MT, Nixon C, Liu E, Mah LY, Ryan KM. Analysis of macroautophagy by immunohistochemistry. Autophagy. 2012; 8:963–969. [PubMed: 22562096]

Ruchaud S, Korfali N, Villa P, Kottke TJ, Dingwall C, Kaufmann SH, Earnshaw WC. Caspase-6 gene disruption reveals a requirement for lamin A cleavage in apoptotic chromatin condensation. EMBO J. 2002; 21:1967–1977. [PubMed: 11953316]

Saidi LJ, Polydoro M, Kay KR, Sanchez L, Mandelkow EM, Hyman BT, Spires-Jones TL. Carboxy terminus heat shock protein 70 interacting protein reduces tau-associated degenerative changes. J Alzheimers Dis. 2015; 44:937–947. [PubMed: 25374103]

Schaeffer V, Lavenir I, Ozcelik S, Tolnay M, Winkler DT, Goedert M. Stimulation of autophagy reduces neurodegeneration in a mouse model of human tauopathy. Brain. 2012; 135:2169–2177. [PubMed: 22689910]

Scholl M, Lockhart SN, Schonhaut DR, O'Neil JP, Janabi M, Ossenkoppele R, Baker SL, Vogel JW, Faria J, Schwimmer HD, Rabinovici GD, Jagust WJ. PET Imaging of Tau Deposition in the Aging Human Brain. Neuron. 2016; 89:971–982. [PubMed: 26938442]

Shalini S, Dorstyn L, Dawar S, Kumar S. Old, new and emerging functions of caspases. Cell Death Differ. 2015; 22:526–539. [PubMed: 25526085]

Simon DJ, Weimer RM, McLaughlin T, Kallop D, Stanger K, Yang J, O'Leary DD, Hannoush RN, Tessier-Lavigne M. A caspase cascade regulating developmental axon degeneration. J Neurosci. 2012; 32:17540–17553. [PubMed: 23223278]

Slee EA, Adrain C, Martin SJ. Executioner caspase-3, -6, and -7 perform distinct, non-redundant roles during the demolition phase of apoptosis. J Biol Chem. 2001; 276:7320–7326. [PubMed: 11058599]

Stratmann K, Heinsen H, Korf HW, Del Turco D, Ghebremedhin E, Seidel K, Bouzrou M, Grinberg LT, Bohl J, Wharton SB, den Dunnen W, Rub U. Precortical phase of Alzheimer's disease (AD)-related tau cytoskeletal pathology. Brain Pathol. 2015

Suemoto CK, Ferretti-Rebustini RE, Rodriguez RD, Leite RE, Soterio L, Brucki SM, Spera RR, Cippiciani TM, Farfel JM, Chiavegatto Filho A, Naslavsky MS, Zatz M, Pasqualucci CA, Jacob-Filho W, Nitrini R, Grinberg LT. Neuropathological diagnoses and clinical correlates in older adults in Brazil: A cross-sectional study. PLoS Med. 2017; 14:e1002267. [PubMed: 28350821]

Terry RD, Masliah E, Salmon DP, Butters N, DeTeresa R, Hill R, Hansen LA, Katzman R. Physical basis of cognitive alterations in Alzheimer's disease: synapse loss is the major correlate of cognitive impairment. Ann Neurol. 1991; 30:572–580. [PubMed: 1789684]

Theofilas P, Polichiso L, Wang X, Lima LC, Alho AT, Leite RE, Suemoto CK, Pasqualucci CA, Jacob-Filho W, Heinsen H, Grinberg LT. Brazilian Aging Brain Study Group. A novel approach for integrative studies on neurodegenerative diseases in human brains. J Neurosci Methods. 2014; 226:171–183. [PubMed: 24503023]

Theofilas P, Steinhauser C, Theis M, Derouiche A. Morphological study of a connexin 43-GFP reporter mouse highlights glial heterogeneity, amacrine cells, and olfactory ensheathing cells. J Neurosci Res. 2017

Tomlinson BE, Irving D, Blessed G. Cell loss in the locus coeruleus in senile dementia of Alzheimer type. J Neurol Sci. 1981; 49:419–428. [PubMed: 7217992]

Uribe V, Wong BK, Graham RK, Cusack CL, Skotte NH, Pouladi MA, Xie Y, Feinberg K, Ou Y, Ouyang Y, Deng Y, Franciosi S, Bissada N, Spreeuw A, Zhang W, Ehrnhoefer DE, Vaid K, Miller FD, Deshmukh M, Howland D, Hayden MR. Rescue from excitotoxicity and axonal degeneration accompanied by age-dependent behavioral and neuroanatomical alterations in caspase-6-deficient mice. Hum Mol Genet. 2012; 21:1954–1967. [PubMed: 22262731]

Vilchez D, Saez I, Dillin A. The role of protein clearance mechanisms in organismal ageing and age-related diseases. Nat Commun. 2014; 5:5659. [PubMed: 25482515]

Wang XJ, Cao Q, Zhang Y, Su XD. Activation and regulation of caspase-6 and its role in neurodegenerative diseases. Annu Rev Pharmacol Toxicol. 2015; 55:553–572. [PubMed: 25340928]

Wolfe DM, Lee JH, Kumar A, Lee S, Orenstein SJ, Nixon RA. Autophagy failure in Alzheimer's disease and the role of defective lysosomal acidification. Eur J Neurosci. 2013; 37:1949–1961. [PubMed: 23773064]

Wong E, Cuervo AM. Autophagy gone awry in neurodegenerative diseases. Nat Neurosci. 2010; 13:805–811. [PubMed: 20581817]

Zhang Y, Goodyer C, LeBlanc A. Selective and protracted apoptosis in human primary neurons microinjected with active caspase-3, -6, -7, and -8. J Neurosci. 2000; 20:8384–8389. [PubMed: 11069945]

Highlights

- in the earliest vulnerable brain regions to AD-type neurofibrillary tangles (NFT) (LC and DRN) in AD
- NFT burden correlates with increased caspase-6 activity in AD
- Co-localization of NFT and autophagosomes increases with Braak AD stage progression
- Co-localization of NFT and active caspase-6 increases with Braak AD stage progression
- Modulation of autophagy and caspase pathways in AD may have potential therapeutic benefits

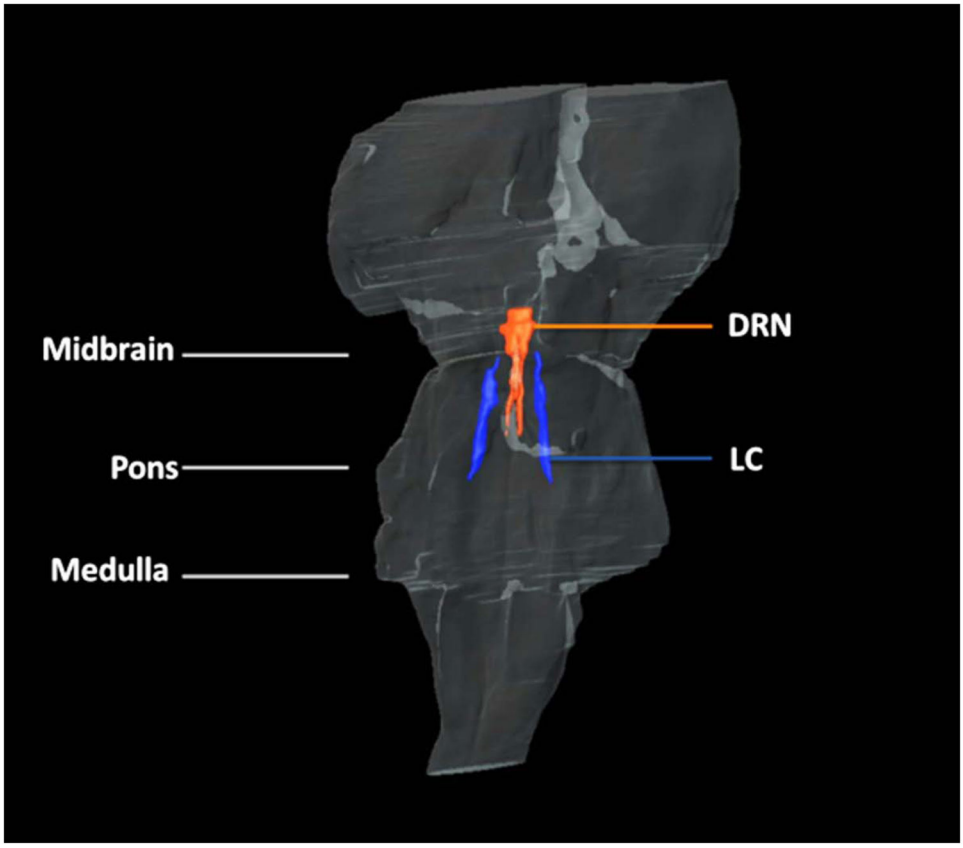

Figure 1. 3D volume reconstruction of the locus coeruleus (LC) and dorsal raphe nucleus (DRN) of the human brainstem

Serial histological sections of the brainstem were used to reconstruct the volume of LC (blue) and DRN (red) using advanced graphics software. The transparent surface represents the brainstem boundaries. The two aminergic nuclei are one of the earliest brain regions affected by tau pathology in individuals with AD.

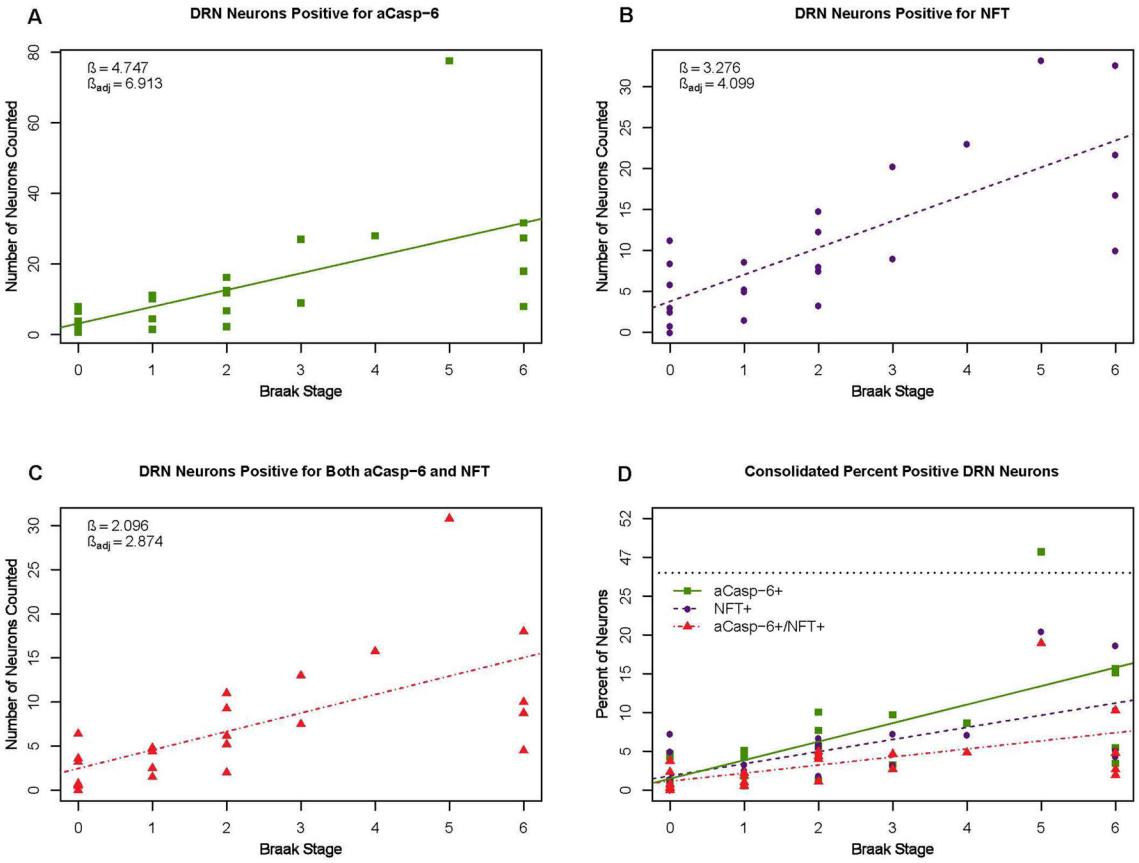

Figure 2. Scatterplots of active Casp-6 and neurofibrillary tangle positivity in neurons of the DRN

(A) A significant positive association was detected between BB stage and the number of DRN neurons positive for aCasp-6 (β=4.747; p=0.001; 95% CI [2.146, 7.349]). After age adjustment, the association remains significant (β= 6.913; p>0.001; 95% CI [3.846, 9.979]). (B) A significant positive association was detected between BB stage and the number of DRN neurons positive for NFTs (β=3.276; p>0.001; 95% CI [2.069, 4.482]). After age adjustment, the association remains significant (β=4.099; p>0.001; 95% CI [2.617, 5.580]). (C) A significant positive association was detected between BB stage and the number of DRN neurons positive for both aCasp-6 and NFTs (β= 2.096; p>0.001; 95% CI [1.026, 3.166]). After age adjustment, the association remains significant (β= 2.876; p>0.001; 95% CI [1.575, 4.174]. (D) Models for the percent of neurons positive for only aCasp-6 (square), only NFT (circle), and co-localization for the two (triangle) were significant (β=2.387; p=0.007; 95% CI [0.723, 4.050], β=1.564; p>0.001; 95% CI [0.787, 2.340], and β=1.04 p=0.004; 95% CI [0.366, 1.713], respectively). After age adjustment, values remained significant (β=4.027; p>0.001; 95% CI [2.171, 5.883]), β=2.341; p>0.001; 95% CI [1.480, 3.202], and β=1.698; p>0.001; 95% CI [0.944, 2.452], respectively).

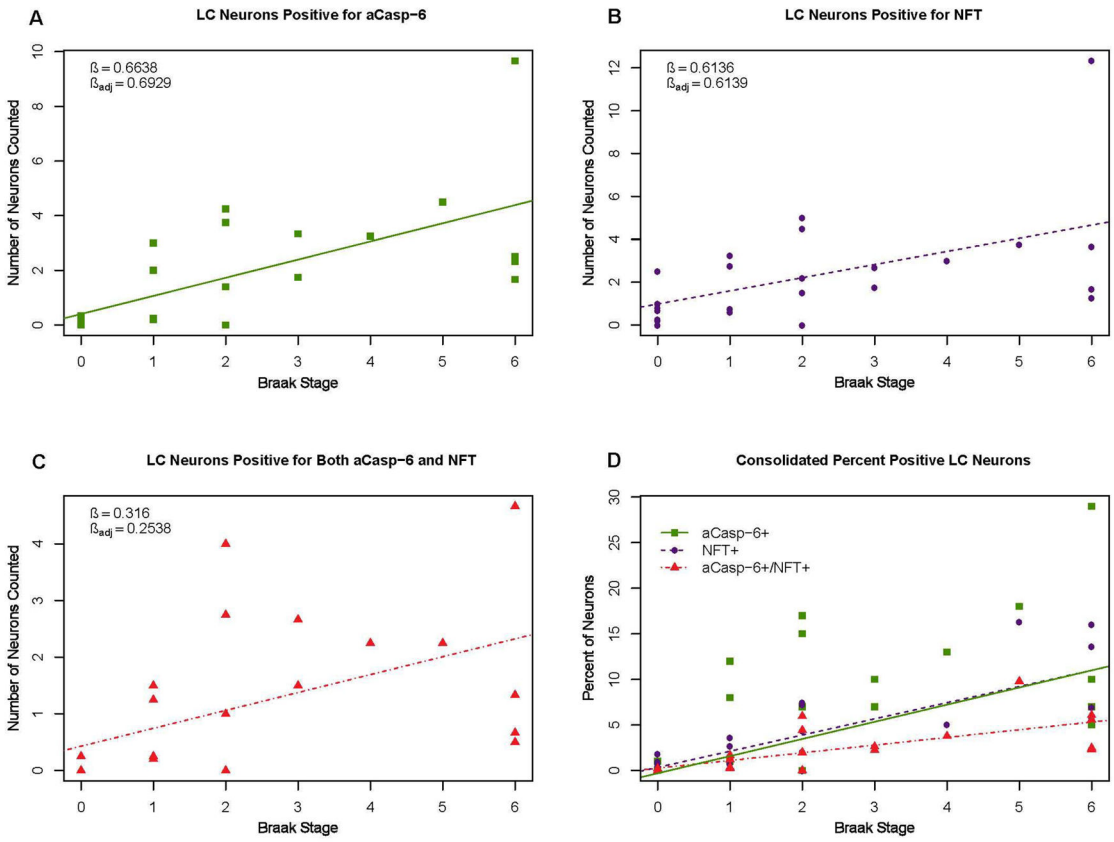

Figure 3. Scatterplots of active Casp-6 and neurofibrillary tangle positivity in neurons of the LC

(A) A significant positive association was detected between BB stage and the number of LC neurons positive for aCasp-6 (β=0.664 cells; p>0.001; 95% CI [0.316, 1.012]). After age adjustment, the association remains significant (β= 0.693 cells; p=0.005; 95% CI of [0.233, 1.153]). (B) A significant positive association was detected between BB stage and the number of LC neurons positive for NFT (β=1.883; p>0.001; 95% CI [1.292, 2.473]). After age adjustment, the association remains significant (β=0.614; p=0.041; 95% CI [0.027, 1.200]). (C) A significant positive association was detected between BB stage and the number of LC neurons positive for both aCasp-6 and NFT (β=0.316; p=0.01; 95% CI [0.082, 0.550]). After age adjustment, the association lost significance (β=0.254; p=0.1; 95% CI [−0.053, 0.560]). (D) Models for the percent of neurons positive for only aCasp-6 (square), only NFT (circle), and co-localization for the two (triangle) were significant (β=1.883; p>0.001; 95% CI [1.292, 2.473], β=1.776; p>0.001; 95% CI [1.177, 2.375], and β=0.844; p>0.001; 95% CI [0.472, 1.217], respectively). After age adjustment, values remained significant (β=2.395; p>0.001; 95% CI [1.707, 3.084], β=2.335; p>0.001; 95% CI [1.653, 3.017], and β=0.984; p>0.001; 95% CI [0.501, 1.467], respectively).

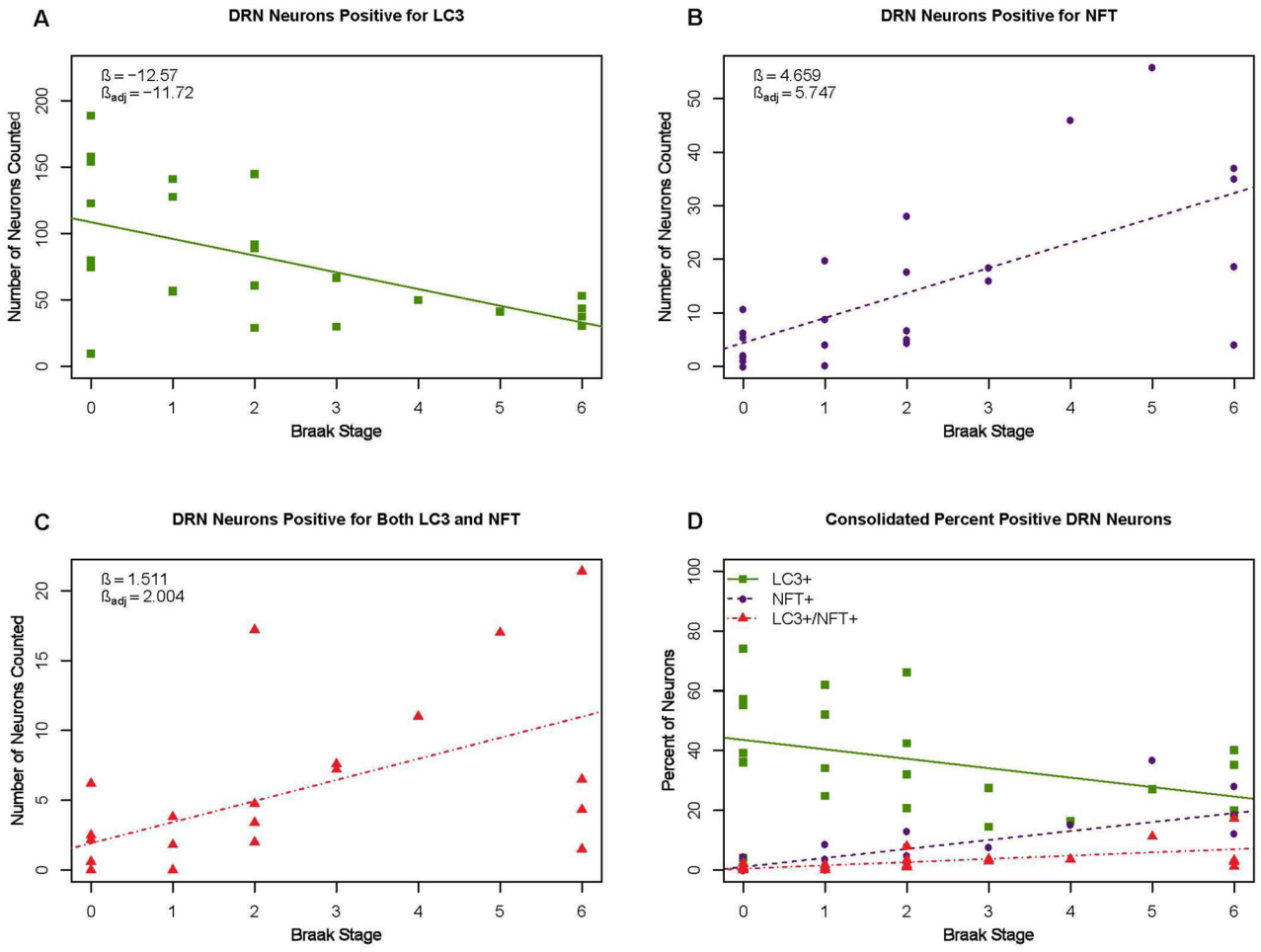

Figure 4. Scatterplots of LC3 and neurofibrillary tangle marker positivity in neurons of the DRN

(A) A significant negative association was detected between BB stage and the number of DRN neurons positive for LC3 (β=−12.573; p=0.004; 95% CI [−20.860, −4.287]) that remained significance after age adjustment (β=−11.723; p=0.036; 95% CI [−22.663, −0.782]). (B) A significant positive association was detected between BB stage and the number of DRN neurons positive for NFT (β=4.659; p>0.001; 95% CI of [2.318, 6.999] and remained significant after adjusting for age (β=5.747; p>0.001; 95% CI [2.753, 8.741]). (C) A significant positive association was detected between BB stage and the number of DRN neurons positive for both LC3 and NFT (β=1.511; p=0.004; 95% CI [0.528, 2.493]) that remained significance after adjusting for age (β=2.004; p=0.003; 95% CI [0.754, 3.254]). (D) The models for the percent of neurons positive for only NFT (circle) and the percent colocalized for the LC3/NFT (triangle) were significant (β=2.99; p>0.001; 95% CI [1.68, 4.31] and β=1.08; p=0.002; 95% CI [0.43, 1.74], respectively). When these models were adjusted for age, they remained significant (β=4.38; p>0.001; 95% CI [1.67, 3.87] and β=1.76; p=0.001; 95% CI [0.97, 2.54], respectively). Neither the unadjusted or age adjusted models for the interaction between the percentages of neurons positive for only LC3 in the DRN (square) were significant (unadjusted: β=−3.16; p=0.129; 95% CI [−6.83, 0.94]; adjusted: β=−3.81; p=0.274; 95% CI [−8.83, 1.20]).

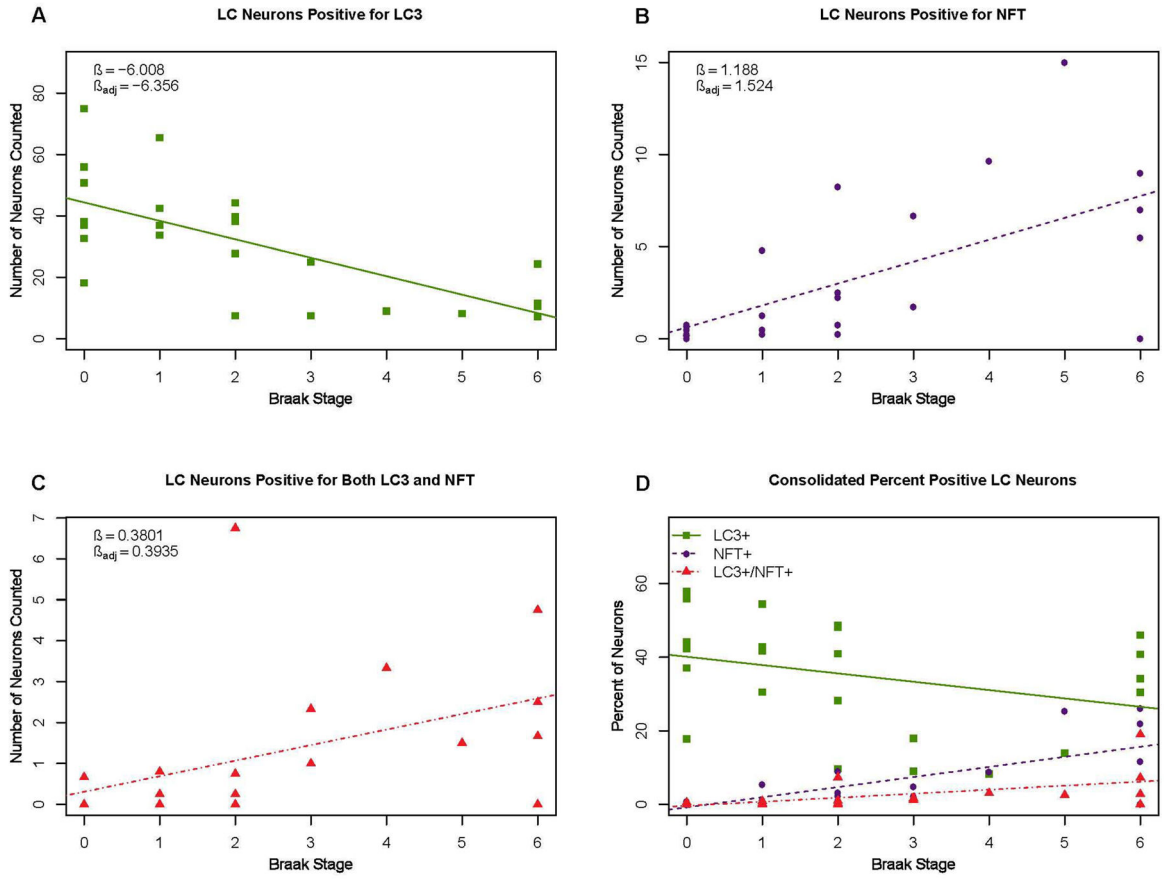

Figure 5. Scatterplots of LC3 and neurofibrillary tangle marker positivity in neurons of the LC

(A) A significant negative association was detected between BB stage and the number of LC neurons positive for LC3 (β=−6.01; p>0.001; 95% CI [−8.83, −3.19] and remains significant after adjusting for age (β=−6.36; p=0.002; 95% CI [−10.07, −2.64]).

(B) A significant positive association was detected between Braak stage and the number of LC neurons positive for NFT (β=1.19; p=0.001; 95% CI [0.56, 1.82]) and remained significant when the model is adjusted for age (β=1.52; p>0.001; 95% CI [0.72, 2.32]). (C) A significant association was detected between BB stage and the number of LC neurons positive for both LC3 and NFT (β=0.38; p=0.016; 95% CI [0.08, 0.68], but lost significance after age adjustment: β=0.39; p=0.05; 95% CI [−0.01, 0.79]). (D) Models for the percent of neurons positive only NFT (circle) and co-localization of NFT and LC3 (triangle) were significant β=2.74; p>0.001; 95% CI [1.63, 3.84], and β=1.09; p=0.003; 95% CI [0.4, 1.78], respectively). When the models were adjusted for age, they remained significant (β=4.02; p>0.001; 95% CI [2.88, 5.15], and β= 1.61; p>0.001; 95% CI [0.78, 2.44], respectively). No significant association was detected between Braak stage and the number of LC neurons positive for only LC3 (square) (unadjusted: β=−2.26; p=0.12; 95% CI [−5.17, 0.65], adjusted: β=−1.83; p=0.33; 95% CI [−5.67, 2.01])

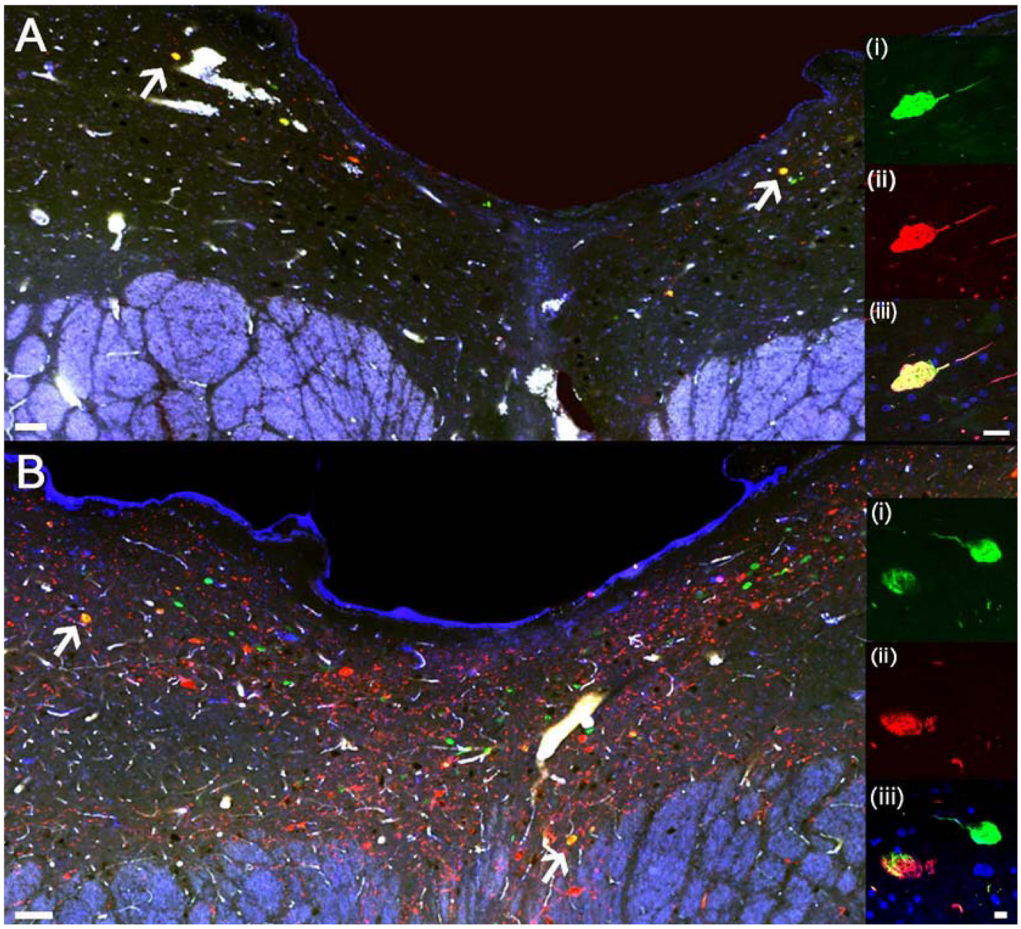

Figure 6. Active Casp-6 positive neurons accumulate and co-localize with neurofibrillary tangles in the DRN of control and AD human brains

Multiple fluorescent staining of aCasp-6 (green; insets A (i), B (i)) and CP-13 (red; insets A (ii), B (ii)) and DAPI (blue) from control individuals (A) and individuals late stages of AD (B) showed positivity in neurons of the DRN. Note the difference in the red and green channels for the control versus late AD brains, the later having a much stronger immunoreactivity for both markers. Neurons with aCasp-6 and CP-13 co-localization (orange; arrows A and B; insets A (iii), B (iii)) suggest the involvement of aCasp-6 in tau-induced pathology. Note the overlapping of the two markers in the neuronal cytoplasm and processes (insets A (iii), B (iii)). Scale bar insets: (A) 20 μm; (B) 40 μm.

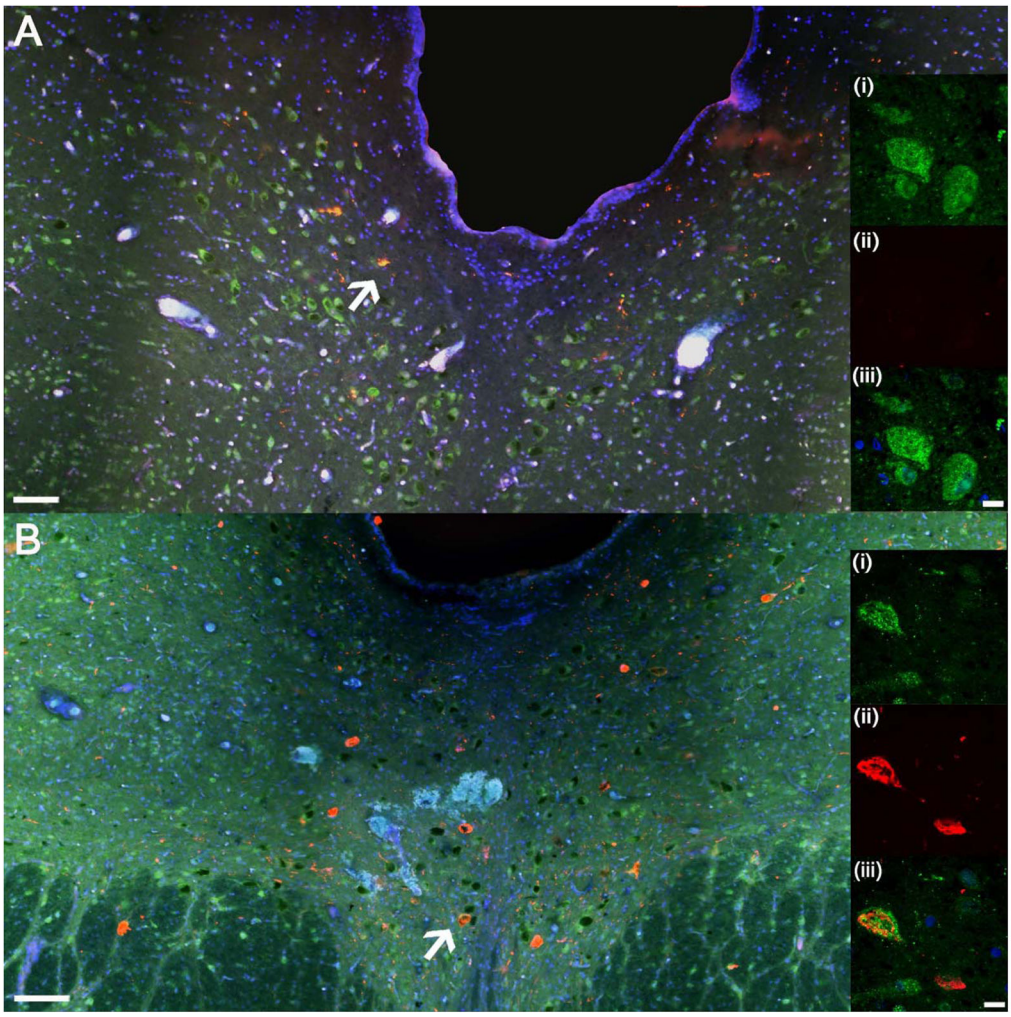

Figure 7. Neurons positive for the macroautophagy marker LC3 show also positivity for neurofibrillary tangles in the DRN of control and AD human brains

Immunofluorescent staining of LC3 (green; insets A (i), B (i)) and CP-13 (red; insets A (ii), B (ii)) and DAPI (blue) from control individuals (A) and individuals late stages of AD (B) showed positivity in neurons of the DRN. Note the difference in the red and green channels for the control versus late AD brains, the latter having fewer cells positive for LC3 but strong immunoreactivity for phospho-tau. Neurons with LC3 and CP-13 colocalization (orange; arrows A and B; insets A (iii), B (iii)) suggest a role of macroautophagy in tau-induced pathology, possibly by defective tau clearance with advancing BB stage. Note the puncta positivity in the cytoplasm B (i), (iii) and the colocalization of the two markers in cell bodies (insets A (iii), B (iii)). Scale bars insets: (A) 10 μm; (B) 10 μm.

Neurobiol Aging. Author manuscript; available in PMC 2019 January 01.

Table 1

Characteristics of the subjects

Subjects	Braak stage	Age (y)	CERAD score	Gender	NIA-AA scores	Education (y)	Brain Weight (Grams)	Clinical Dementia Rating	Post Mortem Interval (PMI) Hr:Min
1	0	49	no NP	M	Not ADNC	0	1410	0	16:20
2	0	58	no NP	M	Not ADNC	4	1168	0	18:55
3	0	47	no NP	F	Not ADNC	5	1202	0	12:00
4	0	65	no NP	F	Not ADNC	4	1020	0	16:15
5	0	44	no NP	F	Not ADNC	10	n/a	0	13:30
6	0	49	no NP	F	Not ADNC	11	1222	0	18:25
7	0	66	no NP	M	Not ADNC	4	1292	0	15:45
8	1	62	scarce	M	Low ADNC	4	1100	0	11:20
9	1	59	scarce	M	Low ADNC	5	1170	0	13:05
10	1	55	no NP	M	Not ADNC	13	1306	0	14:55
11	1	65	no NP	F	Not ADNC	4	1204	0	13:48
12	2	77	scarce	F	Low ADNC	11	1028	0	10:44
13	2	70	scarce	F	Low ADNC	4	1136	0	16:25
14	2	69	scarce	M	Low ADNC	2	1180	0	17:31
15	2	71	scarce	M	Low ADNC	11	1040	0	9:53
16	2	71	no NP	F	Not ADNC	0	1002	0	16:10
17	3	76	moderate	M	Intermediate ADNC	n/a	1166	3	15:35
18	3	77	moderate	F	Intermediate ADNC	4	1130	0	14:45
19	4	83	frequent	F	High ADNC	15	1202	0	11:07
20	5	54	frequent	F	High ADNC	4	1202	3	20:20
21	6	78	frequent	F	High ADNC	4	1080	3	17:20
22	6	60	frequent	M	High ADNC	16	1140	3	05:12
23	6	88	frequent	F	High ADNC	0	1052	2	14:00
24	6	82	frequent	M	High ADNC	16	1133	3	06.45

ADNC: Alzheimer's disease neuropathologic changes; CERAD: Consortium to Establish a Registry for Alzheimer's Disease (Mirra et al., 1991) ee. NIA-AA: National Institute on Aging - Alzheimer's Association guidelines for the neuropathologic assessment of AD (Hyman et al., 2012). No NP: no neuritic plaques.

Table 2

List of primary antibodies used in this study

Antibody	Host	Provider	Dilution
Active caspase-6 (Cleaved-Asp179)	Polyclonal Rabbit	Aviva Systems (San Diego, CA). Cat Nr: OAAF05316	1:100
LC3	Polyclonal Rabbit	Novus Biologicals (Littleton, CO). Cat Nr: NB100-2331	1:200
CP-13 (Serine 202)	Monoclonal Mouse	Gift from Peter Davies, NY	1:500

LC3: microtubule-associated protein, 1A/1B-light chain-3

Table 3

Classification of neurons for analysis

Experimental Groups	1	2	3	4
Caspases and NFT *	Casp-6 positive only	NFT positive only	aCasp-6 and NFT positive	Negative for aCasp-6 and NFT
Macroautophagy and NFT *	LC3 positive only	NFT positive only	LC 3 and NFT positive	Negative for LC3 and NFT

aCasp-6: active caspase 6; **LC3:** microtubule-associated protein, 1A/1B-light chain-3;

* detected using CP-13 antibody